Efficient functionalization of gold nanoparticles by cysteine conjugated protoporphyrin IX for singlet oxygen production in vitro

Article *in* RSC Advances · December 2015

DOI: 10.1039/C5RA15862A

CITATIONS
14

READS
60

5 authors, including:

Mohsen Ashjari
University of Kashan
26 PUBLICATIONS **370** CITATIONS
SEE PROFILE

Daryoush Fatehi
Shahrekord University of Medical Sciences
57 PUBLICATIONS **439** CITATIONS
SEE PROFILE

Ronak Shabani
Iran University of Medical Sciences
20 PUBLICATIONS **64** CITATIONS
SEE PROFILE

Morteza Koruji
Iran University of Medical Sciences
74 PUBLICATIONS **747** CITATIONS
SEE PROFILE

RSC Advances

PAPER

Cite this: *RSC Adv.*, 2015, **5**, 104621

Efficient functionalization of gold nanoparticles using cysteine conjugated protoporphyrin IX for singlet oxygen production *in vitro*†

Mohsen Ashjari,*[ab] Soheila Dehfuly,[b] Daryoush Fatehi,[c] Ronak Shabani[d] and Morteza Koruji[d]

Received 7th August 2015
Accepted 18th November 2015

DOI: 10.1039/c5ra15862a

www.rsc.org/advances

Gold nanoparticles with suitable properties are supreme therapeutic agents and provide effective signal enhancement in photodynamic therapy (PDT). In this study, protoporphyrin IX (PpIX) conjugated gold nanoparticles (GNPs) were prepared using covalent conjugation with cysteine as the adaptable linkage. The thiol group of cysteine was bound to the gold nanoparticles and also the formation of the amide linkage between PpIX and cysteine was confirmed using FT-IR. The spectroscopic characterizations (FT-IR and UV-vis) proved the formation of the PpIX conjugated gold nanoparticles. The reaction process was also followed using thin layer chromatography. Two different laser sources were used to activate the PpIX molecule in the ground state which was highly associated with the amount of singlet oxygen produced. Gold nanoparticles revealed a significant improvement in the singlet oxygen production of the PpIX molecule. The photocytotoxicity of the PpIX conjugated gold nanoparticles was also investigated using spermatogonial cells *in vitro*. The results confirm that the designed PpIX conjugated gold nanoparticles have provided a highly efficient agent for cellular photodynamic therapy.

1. Introduction

Photodynamic therapy (PDT) is a nondestructive medical treatment approach which terminates cancerous and abnormal cells using a combination of a photosensitizing molecule and light irradiation at a wavelength appropriate to the production of reactive oxygen species.[1–3] The photosensitizing molecule becomes excited and then its energy is transferred to ground state molecular oxygen to produce reactive oxygen species (ROS) such as singlet oxygen ($^1O_2$). Singlet oxygen can cause the oxidation of amino acids, DNA, and lipids, leading to cell destruction which forms the basis of PDT for cancer treatment.[4] The effectiveness of PDT has been determined by the efficiency of the singlet oxygen production.[5] Many factors influence singlet oxygen production such as the nature of the photosensitizer, the light wavelength, the light intensity and so on.[6]

Nanotechnology has revolutionised PDT applications, as nanoparticles *e.g.* gold nanoparticles (GNPs) can be used as multi-functional medicines.[7] Due to the large enhancement of the surface electric field on the metal nanoparticles' surface, many applications such as PDT are possible. One of the main features of metal nanoparticles is their strong surface plasmon resonance (SPR) showing great promise for PDT.

The surface plasmon oscillation is a collective oscillation of the electrons in the conduction band. For gold nanoparticles the oscillation frequency is usually in the visible region giving rise to the strong surface plasmon resonance absorption. The plasmon resonance absorption has an absorption coefficient that is orders of magnitude greater than that of strongly absorbing dyes.[8]

Cysteine [cys, HS–CH_2–CH(NH_2)–COOH] has an especially high affinity for gold due to its thiol (sulfhydryl) side chain, which enables the bonding of drugs to metal surfaces as a crosslinker. In combination with gold nanoparticles, it still retains biofunctionality through the amine and carboxylic groups. Functionalization of gold nanoparticles with cysteine leads to the aggregation of nanostructures which is generally attributed to the formation of zwitterions involving the interaction of the deprotonated carboxylate and protonated amine groups of one cys-GNP with the opposite groups of cysteine absorbed on adjacent nanoparticles. Cysteine adsorbs as a fully protonated cation when deposited from acidic solutions and as the fully deprotonated anion in basic solutions.[9] A large number of synthetic routes are suitable for the preparation of gold

[a]*Chemical Engineering Department, Faculty of Engineering, University of Kashan, Kashan, Iran. E-mail: ashjari.m@kashanu.ac.ir; ashjari.m@gmail.com; Fax: +98 31 55912424; Tel: +98 31 55912494*

[b]*Institute of Nanoscience and Nanotechnology, University of Kashan, Kashan, Iran. E-mail: s.dehfuly65@gmail.com*

[c]*Medical Physics Department, Faculty of Medicine, Shahrekord University of Medical Sciences, Shahrekord, Iran. E-mail: d.fatehi@yahoo.com*

[d]*Cellular and Molecular Research Center & Department of Anatomical Sciences, School of Medicine, Iran University of Medical Sciences, Tehran, Iran. E-mail: ronakshabani@yahoo.com; koruji1@gmail.com*

† Electronic supplementary information (ESI) available. See DOI: 10.1039/c5ra15862a

nanoparticles in a controlled manner.[10–12] Firstly Turkevich has demonstrated the synthesis of gold nanoparticles with a diameter of 20 nm *via* the reduction of $HAuCl_4$ by trisodium citrate.[13] Sarangi *et al.* have studied the fluorescence properties of gold nanoparticles capped with cysteine obtained by direct chemical reduction in the presence of amino acids.[14]

Protoporphyrin IX (PpIX) is a model photosensitizing drug which has an absorption maximum of 410 nm (Soret band), along with four smaller peaks near 510, 540, 580 and 635 nm (Q bands), allowing for irradiation from multiple light sources with diverse spectral yields.[15] The carboxyl groups of PpIX play an important role in bioconjugation. Since the carboxyl groups are not directly attached to the porphyrin ring, due to conjugation, the esterification of these groups has no direct effect on the electron distribution in the porphyrin ring and induces a significant change in the light absorption and fluorescence spectra.[16]

The tunable surface properties of gold nanoparticles allow the binding and carrying of photosensitizers attached to their surface by covalent or non-covalent bonds and improve singlet oxygen production. Conjugation of photosensitizers onto the surface of gold nanoparticles was introduced by Hone *et al.* in 2002.[17] They have coated gold nanoparticles with a phthalocyanine photosensitizer which was shown to produce singlet oxygen with enhanced efficiency as compared to the free phthalocyanine. In an *in vitro* study, Gamaleia *et al.* reported that the PDT activity of hematoporphyrin–gold nanoparticles is much higher than that of the original photosensitizer.[18] Ganesan *et al.* used glutathione (GSH) in the synthesis of gold nanoparticles for the electrostatic and covalent conjugation of PpIX.[6] They have conjugated folic acid to carry their complex and indicated that the nanoparticle complexes are more phototoxic compared to free PpIX. Also they revealed that the covalent complex is better than the other complexes and the folate-mediated nanocomplex is the best of the studied complexes.[6] Eshghi *et al.* have described an efficient drug vector to deliver photosensitizers into cells *via* the synthesis of PpIX gold nanoparticle conjugates. They functionalized gold nanoparticles' surfaces with 6-mercapto-1-hexanol in order to attach the PpIX molecule.[19] Yang *et al.* have demonstrated that due to increasing plasmon strength, the conjugation of PpIX onto gold nanoparticles' surfaces enhanced ROS production.[4] Recently, they explored gold nanoparticle aggregates for improving PDT efficiency *in vitro* which can be formed *via* electrostatic interactions. They reported that ROS production by PpIX in the presence of aggregates was two times higher than that for free PpIX.[5] Hayden *et al.* studied electrostatic complexes with a plasmonic effect on PpIX activity by applying rigid surface attachment using gold nanospheres and nanorods.[20] They found that when PpIX is covalently bound close to the spherical nanoparticle surface, the best enhancement occurs for photosensitizer activity.

Here, we investigated the relative increase in the PDT efficacy caused by conjugating PpIX to modified gold nanoparticles, using cysteine as a proper linker. We have synthesized cysteine modified gold nanoparticles (cys-GNPs) and we used a covalent binding technique to conjugate PpIX onto the surface of the gold nanoparticles. Furthermore, we have studied the singlet oxygen production and PDT efficacy of the synthesized PpIX-conjugated cysteine-modified gold nanoparticles (PpIX-cys-GNPs) using a fluorescent probe (anthracene) and spermatogonial cells *in vitro*, respectively.

2. Experimental section

2.1. Materials

Hydrogen tetrachloroaurate(III) trihydrate ($HAuCl_4 \cdot 3H_2O$) 99.5%, L-cysteine, trisodium citrate and anthracene were obtained from Merck Millipore. Protoporphyrin IX, *N*-hydroxy succinimide (NHS), 1-ethyl-3-(3-dimethylaminopropyl)-carbodiimide hydrochloride (EDC), dimethyl sulfoxide (DMSO) and methyl thiazolyldiphenyl-tetrazolium bromide (MTT) were purchased from Sigma-Aldrich (St Louis, MO, USA). Deionized water was used in all aqueous solutions and rinsing procedures. All other chemicals and solvents were analytical grade and used without further purification.

2.2. Preparation of cysteine modified gold nanoparticles (cys-GNPs)

Gold nanoparticles were prepared by a reduction of $HAuCl_4$ using trisodium citrate as the reducing and then stabilizing agent.[13] Briefly, 12.5 mL of sodium citrate solution (38.8 mM) was quickly introduced to 125 mL of a freshly boiled aqueous solution of 1 mM $HAuCl_4 \cdot 3H_2O$ under vigorous stirring. The solution was heated and stirred for another 15 min, during which time its color changed from pale yellow to wine red. The obtained solution was cooled to room temperature while being stirred continuously until the reduction reaction was complete. In order to modify the surface, 0.1 mL of cysteine solution (2.4 mM) was added to 5 mL of the solution and the mixture was stirred for 4 h without any change in color. Finally gold nanoparticles functionalized with cysteine (cys-GNPs) were kept and stored at R.T. for further conjugation.

2.3. Preparation of PpIX conjugated gold nanoparticles (PpIX-cys-GNPs)

In order to chemically conjugate PpIX to the amine group of cysteine on the surface of the gold nanoparticles, activation of the carboxyl group of PpIX is needed.[5] First, 1 mg of PpIX was dissolved in 3 mL of DMSO, followed by the addition 2.3 mg of EDC and 1.7 mg of NHS into the solution. After the complete dissolution, 5 mL of the solution of cys-GNPs was added to the stirring mixture and the reaction was allowed to continue overnight at room temperature forming water-dispersable PpIX-cys-GNP conjugates which were stored at 25 °C for further characterization.

2.4. The singlet oxygen measurement

To detect and qualitatively measure the singlet oxygen level, a fluorescent probe, anthracene, was used. This probe is fluorescent; however it turns into non-fluorescent anthraquinone after being oxidized by singlet oxygen. Initially, anthracene (0.4 mg) was dissolved in methanol (10 mL) at 50 °C. Then 100 μL of the anthracene solution (0.1 mM) was introduced to 3 mL of the

free PpIX solution and the water-dispersed PpIX-cys-GNP conjugates for 60 min before irradiation. In the next step the solutions were placed under L530 (solid-state laser, green) and L633 (gaseous HeNe laser, red) light irradiation with a fixed power density (5 and 17 mW respectively) for 20 min. The samples were further incubated for 20 min at ambient temperature and then the emission spectrum of the anthracene was recorded using a photoluminescence spectrometer. The amount of singlet oxygen produced was measured using the decreasing fluorescence intensity.

2.5. Experimental animals

In this experiment, 20 neonatal mice (3–6 days old) were used. Male neonate National Medical Research Institute (NMRI) mice were obtained from stocks of Razi Laboratory (Tehran, Iran) and moved to the animal house of Iran University of Medical Sciences (Tehran, Iran). They were housed in polycarbonate cages in a room at a temperature range of 22–25 °C, with a 12 hour light/dark cycle. The mice could freely reach drinking water and standard laboratory pellets. National Research Council guidelines were carefully considered during the research.

2.6. Isolation and cultivation of spermatogonial stem cells

Testes from the 3–6 day-old NMRI mice were collected for the preparation of a cell suspension following enzymatic digestions and purification steps. After decapsulation, the testes were minced and suspended in Dulbecco's Modified Eagle Medium/F12 (DMEM/F12) (Gibco, USA) supplemented with 2.438 g L^{-1} $NaHCO_3$, single-strength nonessential amino acids, penicillin (100 IU mL^{-1}), streptomycin (100 μg mL^{-1}), and gentamycin (40 μg mL^{-1}) (all from Life Technologies).

Testicular cells were separated using the method of van Pelt *et al.* (1996) with minor modifications. Briefly, minced testes pieces were suspended in DMEM/F12 containing 0.5 mg mL^{-1} collagenase/dispase, 0.5 mg mL^{-1} trypsin, and 0.05 mg mL^{-1} DNAse, for 30 minutes (with shaking and a little pipetting) at 37 °C. All enzymes were purchased from Sigma-Aldrich. For the next step, the interstitial cells were removed by washing with DMEM/F12 medium and centrifuging for 1 min at 1500 rpm (two–three times). A second digestion step was performed in DMEM/F12 medium by adding a fresh enzyme solution into the seminiferous cord fragments as previously described. After cell separation and filtration through 70 μm nylon filters, the collected cells were used for the culture cells. Sertoli cells and myoid cells were also isolated through overnight differential plating in DMEM/F12 containing 10% fetal calf serum (FCS). After the removal of the Sertoli and myoid cells, spermatogonia, which remained in suspension, were collected and cultured in DMEM/F12 containing 1% FCS and 20 ng mL^{-1} GDNF and bFGF 10 ng mL^{-1} for 2 weeks. The cells were incubated at 32 °C, with 5% CO_2 in a humidified atmosphere, and the medium was refreshed three times per week.

2.7. Cell viability assay

In order to carry out the photocytotoxicity assay spermatogonial cells were divided into four groups: control (no PpIX and no laser irradiation), sham (only laser irradiation), PpIX-cys-GNPs and free PpIX (0.1 mL of 0.125 mg mL^{-1}). After that, the cell viability was evaluated with a MTT assay. Spermatogonial cells were seeded into a 96-well plate at a density of 20×10^3 cells per well per 0.2 mL. To assess the effect of the PpIX activity in the exposure time, the cells were treated with the samples and incubated for 12 hours. After the incubation, all trials (except the control) were irradiated with a HeNe laser (633 nm, 15 mW cm^{-2}) for 20 min. Incubation was continued overnight in dark conditions. Then the cells were centrifuged, and the wells were washed twice with PBS. MTT tetrazolium salt was freshly prepared (5 mg mL^{-1} MTT tetrazolium salt diluted with DMEM/F12 containing 2% FBS). Then 0.2 mL of the prepared solution was added to each well and they were incubated for 4 h at 37 °C, leading to the formation of formazan dye. The solutions were centrifuged and the supernatant was removed. The MTT formazan crystals were then dissolved in DMSO (0.1 mL) for 15 min in a micro titer plate shaker. Afterwards, the optical density (OD) was measured with an ELISA reader (Thermo Electron) at 570 nm as the reference and test wavelength. The viable rate was calculated using the following equation:

$$\text{Viable rate} = (OD_{treated}/OD_{control}) \times 100$$

where $OD_{control}$ was obtained in the absence of laser irradiation and photosensitizer.

2.8. Equipment

The absorbance measurements were performed with a Shimadzu UV-2100 spectrophotometer. FT-IR spectra were recorded on a 102MB BOMEM apparatus. The X-ray diffraction pattern was obtained on an X'Pert pro multipurpose diffractometer (MPD) using Cu-Kα radiation. The morphology and size of the gold NPs was measured on a MIRA3 FEG scanning electron microscope (SEM). Thin-layer chromatography (TLC) was performed using precoated silica gel plates (Merck Kieselgel 60F254). Fluorescence spectra of anthracene were recorded using photoluminescence spectroscopy (Perkin Elmer LS55) at ambient temperature. In order to excite PpIX molecules two illumination sources were used: a helium–neon laser (HNL-150R) and a solid-state laser (MC2000) and then the emitted fluorescence was detected.

3. Results and discussion

The conjugation of PpIX to the cysteine modified gold nanoparticles can be conducted using the EDC/NHS reaction as shown in Fig. 1. An appropriate linkage is necessary for the selective targeting of abnormal cells and to ensure that the photosensitizer conjugates to the nanoparticles efficiently. Cysteine was used to create the linkage between the gold nanoparticles and PpIX. Since cysteine is bifunctional, when it conjugates to nanoparticles it has another functional group for attaching a tumor-specific ligand, such as folic acid. Conjugation of PpIX to GNPs was followed using TLC. Monitoring the conjugation using TLC analysis indicated the progressive disappearance of the PpIX and the formation of the PpIX-cys-

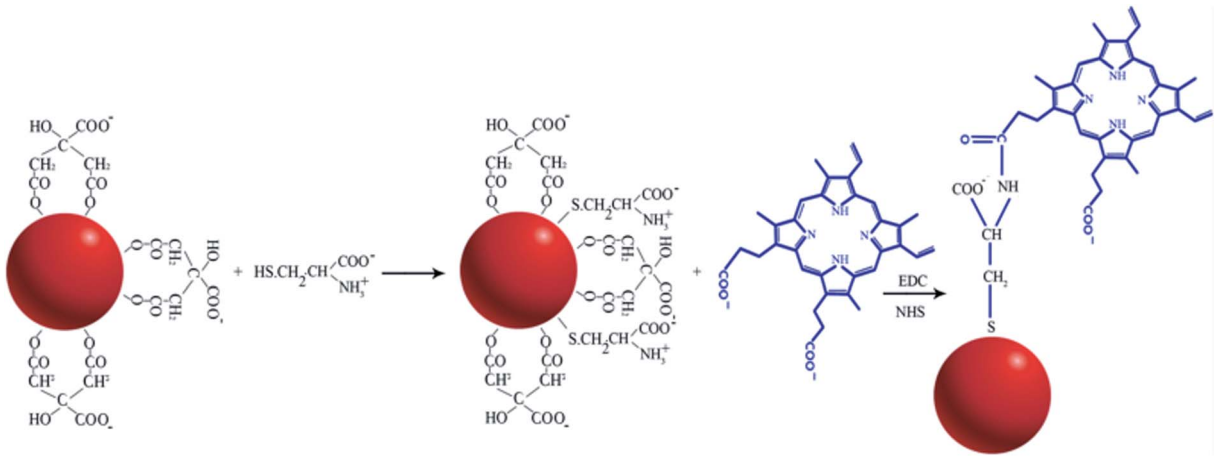

Fig. 1 Schematic illustration of the conjugation of PpIX to a cysteine modified gold nanoparticle.

GNPs. When PpIX conjugates to GNPs, because of the heavy gold nanoparticles attached, PpIX-cys-GNPs molecules are not present on the TLC analysis.

3.1. XRD and SEM analysis of gold nanoparticles

X-ray diffraction (XRD) analysis has been used to study the structure of the prepared gold nanoparticles. Fig. 2a shows a representative XRD pattern of the gold nanoparticles prepared by using trisodium citrate as a reducing agent. The XRD peaks are found to be broad indicating the formation of nanoparticles. Four diffraction peaks are observed which can be indexed to the (111), (200), (220) and (311) reflections of the face centered cubic (fcc) structure of metallic gold. Moreover, the intensity of the (111) diffraction was much stronger than that of the (220), (200) and (311) diffractions. The XRD pattern thus clearly reveals that the synthesized gold nanoparticles were essentially crystalline. However, there were no impurities in the pattern (Fig. 2a). The average particle size of the gold nanoparticles can be calculated using the Debye–Scherrer equation and is found to be around 14.1 nm.[21]

Scanning electron microscopy (SEM) has been applied to identify the size, shape, and morphology of gold nanoparticles. The SEM image (Fig. 2b) of the gold nanoparticles demonstrates that almost spherical particles are more abundant than other shapes. Additionally, these nanoparticles were monodisperse and had an average diameter of roughly 20 nm. This result was consistent with the obtained XRD results.

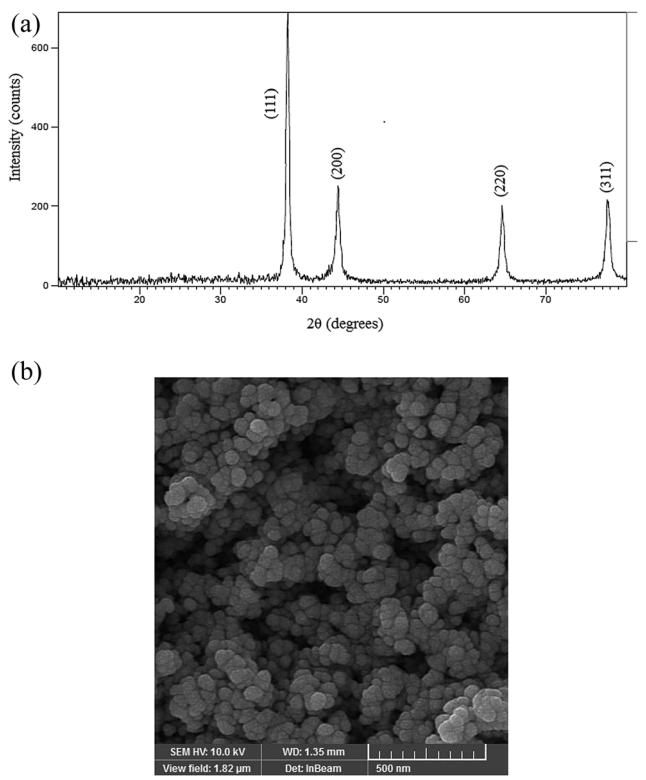

Fig. 2 Structural and morphological analysis of the gold nanoparticles, respectively: XRD pattern (a) and SEM image (b).

3.2. FTIR analysis

The interaction of the prepared gold nanoparticles with cysteine as well as the PpIX conjugation was confirmed using FT-IR spectroscopy as shown in Fig. 3. Cysteine molecules have a characteristic stretching vibration at 2550 cm^{-1}, which is associated with the S–H bond (thiol group). As shown in the FT-IR spectrum of the prepared cys-GNPs (Fig. 3 lower), this peak disappears which is due to the S–H bond breakage. This confirms that the bond formation between the cysteine and gold nanoparticles is from the S head groups. Conjugation of the PpIX molecules on the surface of the modified gold nanoparticles was confirmed by the formation of an amide group in the presence of EDC and NHS as coupling agents and the appearance of its characteristic peaks. Upon covalent bonding of the carboxyl group of the PpIX molecules with the amine groups of the cysteine, the FT-IR spectrum of the PpIX-cys-GNPs (Fig. 3 upper) shows a carbonyl group peak at 1640 cm^{-1} (C=O stretch) and a C–N peak at 1400 cm^{-1} which confirms the formation of an amide bond.

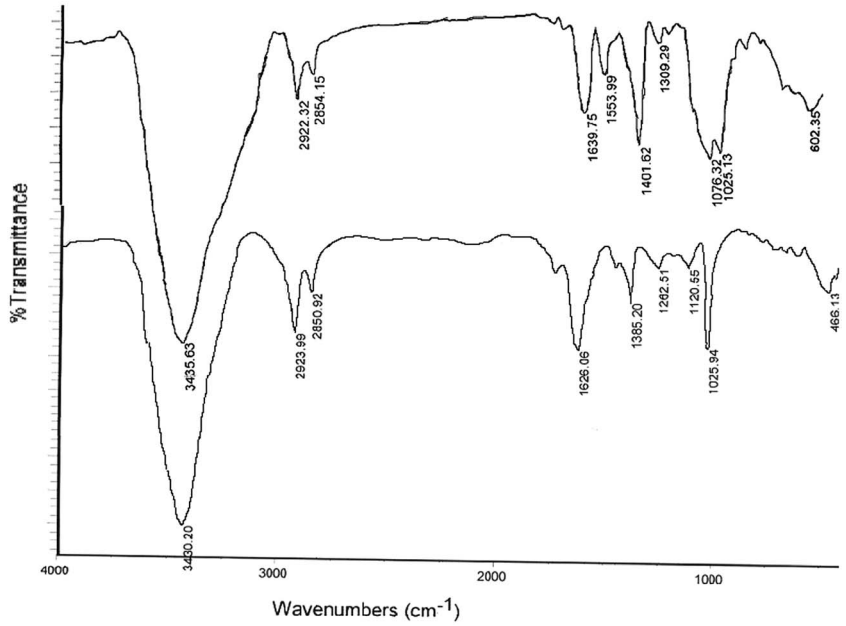

Fig. 3 FT-IR spectra of the cys-GNPs (lower) and PpIX-cys-GNPs (upper).

3.3. UV-vis absorption study

Absorption spectroscopy is an effective method to determine the formation and stability of gold nanoparticles in colloidal aqueous solution. Colloidal solutions of gold nanoparticles have intense colors due to surface plasmon resonance (SPR). The position of the SPR band in UV-vis spectra is sensitive to particle size, shape and local refractive index.[22]

The UV-vis spectrum of the gold nanoparticles synthesized using trisodium citrate in aqueous media is shown in Fig. 4a (curve a). The average particle size of the gold nanoparticles was 14.66 nm which was calculated using the equation proposed by Hiss (5.6×10^{12} gold particles per one liter).[23]

The absorption spectrum of the gold nanoparticles after modification with cysteine (cys-GNPs) is seen in Fig. 4a (curve b). The absorption peak of the cys-GNPs was at 630 nm, which had red-shifted 10 nm in comparison to the absorption peak of the gold nanoparticles. This change might be due to the aggregate size and interparticle distance. When the interparticle distance in the aggregates decreased to less than about the average particle diameter, the electric dipole–dipole interaction and coupling between the plasmons of neighboring particles in the aggregates resulted in the bathochromic shift of the absorption band.[10] In order to study the stability of the cys-GNPs, we analyzed them again after three days (see ESI†) and it was observed that the cys-GNPs were unstable and had aggregated. The positively charged amino group in cysteine ($-NH_3^+$) might interact with the negative charge (COO^-) on the surface of the other gold nanoparticles through electrostatic binding, therefore forming assemblies and aggregates.[10]

The absorption spectra of PpIX and the PpIX-cys-GNPs are shown in Fig. 4b. The absorption spectrum of PpIX has its characteristic peaks at 400 nm, 508 nm, 560 nm and 610 nm.

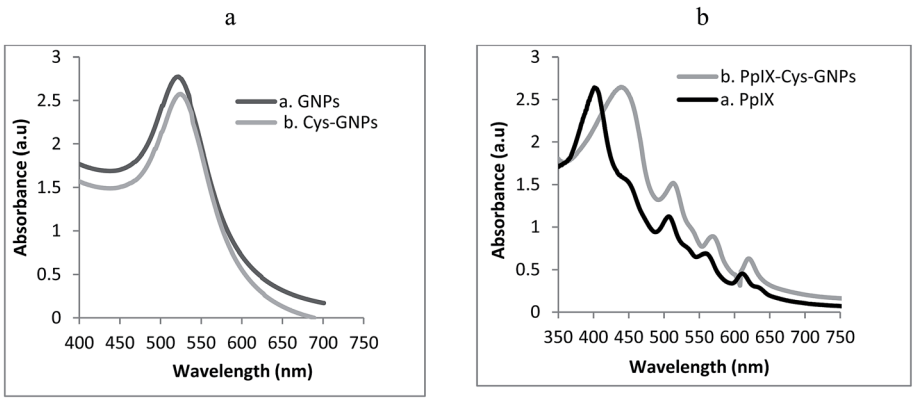

Fig. 4 Absorption spectra of the synthesized samples: (a) gold nanoparticles (dark) and cys-gold nanoparticles (gray), (b) free PpIX (dark) and PpIX-cys-GNP (gray).

The PpIX-cys-GNP conjugate shows that the absorption peaks are red shifted by 25 nm with respect to those in the PpIX spectrum before the conjugation. This red shift could be due to the covalent attachment of the PpIX molecule on the surface of the GNPs. Moreover, it is attributed to the coupling of the individual surface plasmon of the nanoparticles in the aggregated structures, which will be observed if the inter-linked nanostructures are formed.[19] It is also observed that there was an increase in the absorption intensity of some peaks of the PpIX-cys-GNP conjugate with respect to those of the PpIX molecule. This increase might be attributed to the change in the surrounding media and the presence of the amine groups (electron donors).[6] The results agreed with the FTIR analysis and the observed changes in the absorption spectra. Furthermore these results provided indirect evidence of the formation of the PpIX-cys-GNPs.

3.4. Measurement of singlet oxygen

Singlet oxygen production is of great importance in PDT and its measurement presents an indication of how well a photosensitizing molecule is able to produce ROS. To produce suitable singlet oxygen, energy transfer with an efficient rate is required between the excited state of the photosensitizer and the ground state of the oxygen molecules. Anthracene as a singlet oxygen quencher is used to measure the singlet oxygen by changes in the emission spectra when it has been exposed to ROS. The anthraquinone generated has no fluorescence properties in contrast to the anthracene. Actually, the decreasing emission intensity of anthracene represents singlet oxygen production. In order to activate the PpIX molecules, the prepared PpIX-cys-GNPs were stimulated using light sources. For comparison, two light sources, a helium–neon laser (L530 nm) and a solid-state laser (L633 nm), were applied to show efficient energy transfer.

Fig. 5 illustrates the decreasing intensity of anthracene indicating the singlet oxygen produced by the free PpIX and PpIX-cys-GNPs when they were irradiated for 20 min. Evolution of the emission intensity of the anthracene demonstrated that both free PpIX and PpIX-cys-GNPs have produced singlet oxygen. However, the PpIX-cys-GNPs produced more singlet oxygen in comparison with the free PpIX. This could be due to the nature of the chemical binding of the PpIX to the surface of the nanoparticles. Because of the surface plasmon of the gold nanoparticles, highly efficient energy transfer to the PpIX molecule can occur in the ground state, resulting in the excited state, and consequently, the production of singlet oxygen.[20] Thus, using gold nanoparticles is an effective tool for enhancing singlet oxygen production and PDT efficacy.

The effect of the irradiation sources on the singlet oxygen production is shown in Fig. 6. According to this observation, both free PpIX and PpIX-cys-GNPs could adsorb more radiation from L633. This is the result for our prepared conjugate; L633 in comparison with L530 can produce larger amounts of singlet oxygen.

3.5. *In vitro* PDT efficiency

The *in vitro* PDT efficiency of the free PpIX and the PpIX-cys-GNPs was evaluated against spermatogonial cells using the MTT assay technique (MTT, 3-(4,5-dimethylthiazol-2-yl)-2,5-diphenyltetrazolium bromide). The concentrations of the samples were constant (1 g mL^{-1}) and the percentages of photocytotoxicity were determined. It is well-known that cell

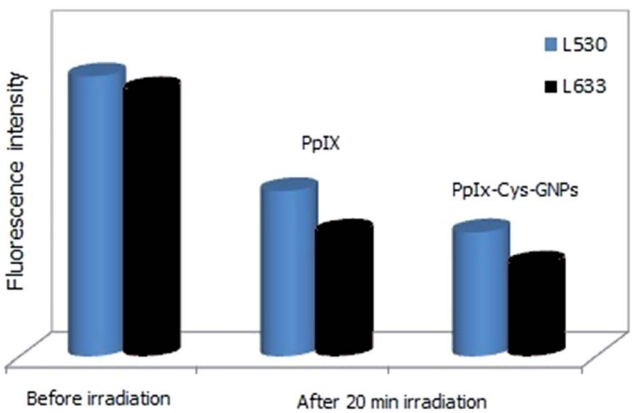

Fig. 6 Different sources (L530 and L633) of irradiation for the samples and the change in the emission intensity of anthracene.

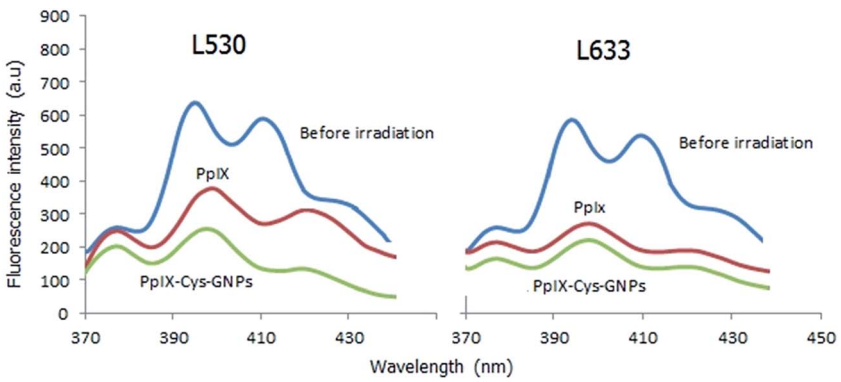

Fig. 5 Reduction of the intensity of anthracene caused by singlet oxygen produced by the PpIX and PpIX-cys-GNPs when they were irradiated by lasers (L530 and L633) for 20 min.

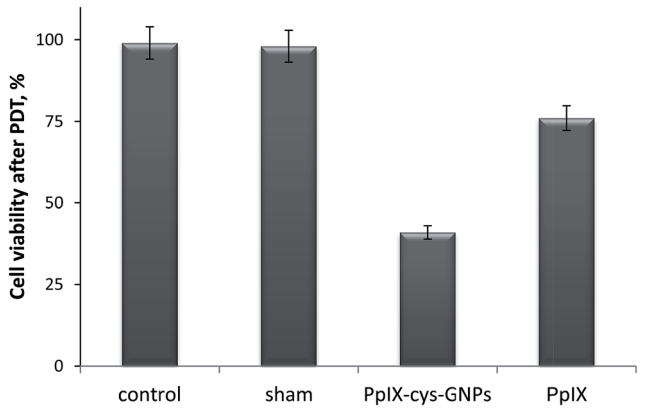

Fig. 7 Viability of spermatogonial cells determined by MTT assay after PDT treatments where cells were incubated with samples for 4 h, and then irradiated for 20 min using a HeNe laser (633 nm, 15 mW cm^{-2}). Subsequently, the cells were cultured for 24 h prior to MTT test.

destruction in PDT treatment is correlated with the singlet oxygen level.[17] With the increase of intracellular singlet oxygen caused by gold nanoparticles, higher cell destruction is expected.

Fig. 7 reveals the photocytotoxic effect of the free PpIX molecules and the PpIX-cys-GNPs. Following PDT, 76% cell viability was observed for the PpIX molecules whereas 41% cell viability was found for the PpIX-cys-GNPs. This could be related to lowering of singlet oxygen production. The control and sham group cells showed a minimal photocytotoxicity effect with a cell viability of 99% and 97% respectively. In this study we found that cells with only light exposure and without any photosensitizer (control and sham samples) demonstrated no detectable photocytotoxicity.

These results confirm that the presence of gold nanoparticles with high plasmonic resonance in PpIX-mediated PDT treatment could significantly enhance the cell destruction efficacy and the PDT efficacy. Moreover, the covalent linkage of the cysteine between the PpIX and gold nanoparticles shows an increase in the photocytotoxic effect, as a result of the stable binding nature; the PDT efficiency is enhanced and hence the cellular uptake is promoted.[5] Further, studies have reported that the stability of the nanoparticle is crucial in enhancing the uptake of the photosensitizer. Conjugation increases the solubility of the PpIX and thereby increases the PDT efficacy.[19]

4. Conclusion

This study shows that gold nanoparticles in combination with cysteine provide a simple way for the conjugation of PpIX and give enhanced PDT efficacy. The preparation of cysteine modified gold nanoparticles was considered using morphological (SEM) and structural (XRD) evaluation techniques and these results proved the formation of the cys-GNPs. TLC analysis indicated that all of the PpIX had been consumed and conjugated to the gold nanoparticles. The cysteine linkage plays an important role in the control of the stabilization of the gold nanoparticles due to the thiol group. The cys-GNPs can be chemically bound with the PpIX molecule. Spectroscopic studies (FT-IR and UV-vis) confirmed bioconjugation between the carboxyl groups of the PpIX molecule and the amine groups on the surface of the metal ion. The singlet oxygen produced was detected by the change in the anthracene spectra. We demonstrated that singlet oxygen production by light irradiation of a PpIX photosensitizer is significantly enhanced by gold nanoparticle conjugates. The PpIX-cys-GNP conjugates were taken up by spermatogonial cells *in vitro* and their photocytotoxicity was also investigated. The designed nanostructured PpIX conjugate has proved to be an efficient agent for PDT which makes it a potential candidate for cancer treatment.

Acknowledgements

This work was funded by the University of Kashan (grant 15190). The authors would like to thank Dr Mehrdad Moradi (University of Kashan) for his assistance in using the laser instrument and his kind cooperation. Authors declare that there is no conflict of interest in this study.

References

1 O. J. Stacey and J. A. S. Pope, *RSC Adv.*, 2013, **3**, 25550.
2 S. S. Lucky, K. C. Soo and Y. Zhang, *Chem. Rev.*, 2015, **115**, 1990.
3 K. Han, J.-Y. Zhu, S.-B. Wang, Z.-H. Li, S.-X. Cheng and X.-Z. Zhang, *J. Mater. Chem. B*, 2015, **3**, 8065–8069.
4 M. Khaing and Y. Yang, *ACS Nano*, 2012, **6**, 1939.
5 Y. Yang, Y. Hu, H. Du and H. Wang, *Chem. Commun.*, 2014, **50**, 7287.
6 S. W. Prasanna, G. Poorani, R. A. Prakasa, M. Elanchezhiyan and S. Ganesan, *J. Nanosci. Nanotechnol.*, 2015, **15**, 5577.
7 D. Bechet, P. Couleaud, C. Frochot, M.-L. Viriot, F. Guillemin and M. Barberi-Heyob, *Trends Biotechnol.*, 2008, **26**, 612.
8 S. Eustis and M. A. El-Sayed, *Chem. Soc. Rev.*, 2006, **35**, 209.
9 A. Ihs and B. Liedberg, *J. Colloid Interface Sci.*, 1991, **144**, 282.
10 R. G. Acres, V. Feyer, N. Tsud, E. Carlino and K. C. Prince, *J. Phys. Chem. C*, 2014, **118**, 10481.
11 S. D. Luthuli, M. M. Chili, N. Revaprasadu and A. Shonhai, *IUBMB Life*, 2013, **65**, 454.
12 A. Majzik, R. Patakfalvi, V. Hornok and I. Dékány, *Gold Bull.*, 2009, **42**, 113.
13 J. Turkevich, *Gold Bull.*, 1985, **18**, 86.
14 S. N. Sarangi, A. M. P. Hussain and S. N. Sahu, *Appl. Phys. Lett.*, 2009, **95**, 073109.
15 A. E. OConnor, W. M. Gallagher and A. T. Byrne, *Photochem. Photobiol.*, 2009, **85**, 1053.
16 *The Porphyrin Handbook*, ed. K. Kadish, R. Guilard and K. Smith, Elsevier, 1st edn, 1999, vol. 2.
17 D. C. Hone, P. I. Walker, R. E. Gowing, S. F. Geral, A. Beeby, I. Chambrier, M. J. Cook and D. A. Russell, *Langmuir*, 2002, **18**, 2985.
18 N. Gamaleia, E. Shishko, G. Dolinsky, A. Shcherbakov, A. Usatenko and V. Kholin, *Exp. Oncol.*, 2010, **32**, 44.

19 H. Eshghi, A. Sazgarnia, M. Rahimizadeh, N. Attaran, M. Bakavoli and S. Soudmand, *Photodiagn. Photodyn. Ther.*, 2013, **10**, 304.
20 S. C. Hayden, L. A. Austin, R. D. Near, R. Ozturk and M. A. El-Sayed, *J. Photochem. Photobiol., A*, 2013, **269**, 34.
21 S. Aswathy and D. Philip, *Spectrochim. Acta, Part A*, 2012, **97**, 1.
22 F. Chai, C. Wang, T. Wang and Z. Ma, *Nanotechnology*, 2010, **21**, 025501.
23 Y. Qiu, S. Liu, L. Kong and Z. Liu, *Spectrochim. Acta, Part A*, 2005, **61**, 2861.